# Effects of hypoxia-reoxygenation on rat blood-brain barrier permeability and tight junctional protein expression

**Ken A. Witt, Karen S. Mark, Sharon Hom, and Thomas P. Davis**
*Department of Pharmacology, College of Medicine, University of Arizona, Tucson, Arizona 85724*

**Witt, Ken A., Karen S. Mark, Sharon Hom, and Thomas P. Davis.** Effects of hypoxia-reoxygenation on rat blood-brain barrier permeability and tight junctional protein expression. *Am J Physiol Heart Circ Physiol* 285: H2820–H2831, 2003. First published August 7, 2003; 10.1152/ajpheart.00589.2003.—Cerebral microvessel endothelial cells that form the blood-brain barrier (BBB) have tight junctions (TJs) that are critical for maintaining brain homeostasis. The effects of initial reoxygenation after a hypoxic insult (H/R) on functional and molecular properties of the BBB and TJs remain unclear. In situ brain perfusion and Western blot analyses were performed to assess in vivo BBB integrity on reoxygenation after a hypoxic insult of 6% $O_2$ for 1 h. Model conditions [blood pressure, blood gas chemistries, cerebral blood flow (CBF), and brain ATP concentration] were also assessed to ensure consistent levels and criteria for insult. In situ brain perfusion revealed that initial reoxygenation (10 min) significantly increased the uptake of [$^{14}$C]sucrose into brain parenchyma. Capillary depletion and CBF analyses indicated the perturbations were due to increased paracellular permeability rather than vascular volume changes. Hypoxia with reoxygenation (10 min) produced an increase in BBB permeability with associated alterations in tight junctional protein expression. These results suggest that H/R leads to reorganization of TJs and increased paracellular diffusion at the BBB, which is not a result of increased CBF, vascular volume change, or endothelial uptake of marker. Additionally, the tight junctional protein occludin had a shift in bands that correlated with functional changes (i.e., increased permeability) without significant change in expression of claudin-3, zonula occludens-1, or actin. H/R-induced changes in the BBB may result in edema and/or associated pathological outcomes.

hypoxemia; occludin; in vivo

---

HYPOXIC INCIDENCE SIGNIFICANTLY influences the blood-brain barrier (BBB) with subsequent effects on neurological tissue. The BBB is a physical and metabolic barrier that separates the peripheral circulation from the central nervous system (CNS) and serves to regulate and protect the microenvironment of the brain. An acute cerebral hypoxic event (i.e., high-altitude exposure, acute pulmonary disease, or clinical or operative hypoxemia) involves a degree of $O_2$ deficiency that is often associated with a loss of metabolic function. An insult of this nature may activate blood and vascular inflammatory mediators, increase reactive $O_2$ species,

and cause edema. Subsequent reoxygenation-associated events have also been shown to be significant contributors to a pathological outcome (21, 35, 52). Clarifying the extent and manner of BBB alterations and delineating the degree of change induced by the hypoxic insult vs. the posthypoxic reoxygenation remain considerable tasks. To understand BBB adaptations during such events, it is necessary to independently examine the contributing factors.

The BBB is formed by a monolayer of microvessel endothelial cells that restricts the movement of small polar molecules and macromolecules between the blood and the brain interstitial fluid. The restrictive nature of the BBB is due to the lack of fenestrations, decreased pinocytotic activity (8), and the presence of tight junctions (TJs), which are domains of occluded intercellular clefts (13, 51) that result in a high transendothelial electrical resistance (1,500–2,000 $\Omega/cm^2$ in pial vessels; Refs. 6, 10). The microvessel endothelial cells that compose the BBB express both functional and regulatory proteins that form the TJs. Perturbations of BBB function can result in dysregulation of brain homeostasis.

In this investigation, we assessed tight junctional proteins of the BBB and focused on the initial posthypoxic reoxygenation state. Although the tight junctional complex is critical for restricting paracellular diffusion in the cerebral microvasculature (33), it is recognized that the BBB is vulnerable to hypoxia-reoxygenation (H/R) injury that ultimately causes increased microvascular permeability and vasogenic edema (24, 48). The tight junctional complex is formed by plasma membrane proteins that are connected to the cytoarchitecture via associated accessory proteins (41). Occludin and claudins [with 20 identified isoforms (62)] are integral transmembrane proteins that homotypically bind with those of adjacent cells to form the tight junctional seal (15, 16). Cytoplasmic tight junctional accessory proteins [zonula occludens (ZO)-1, -2, and -3 and cingulin] connect the transmembrane proteins to the actin cytoskeleton (29, 23). ZOs are membrane-associated guanylate kinase proteins that are critical in forming and stabilizing TJs by binding occludin to the cytoarchitecture (23, 42). ZO-1 is directly linked to the COOH terminus of occludin (17) and is

---

considered to be important for localization of occludin to the TJs (33, 63). To our knowledge, analysis of BBB tight junctional protein expression during posthypoxic reoxygenation has not been conducted in vivo.

Specific focus on $O_2$ supply with regard to the BBB is itself a multifaceted area of research. BBB alteration due to $O_2$ deprivation can be divided into two phases: *1*) the hypoxic insult phase, and *2*) the posthypoxic reoxygenation phase (acute and chronic). The degree of $O_2$ deficit (in %) and the time course of the hypoxic phase as well as the reoxygenation phase are critical in determining the nature and level of BBB alteration. Although hypoxia and posthypoxic reoxygenation stresses have been shown to increase cerebrovascular paracellular permeability with in vitro BBB models (2, 39, 40), the conditions and criteria of stress vary considerably across models. In vitro modeling is essential for examination of particular cellular events and provides an understanding of cellular mechanisms, and an evaluation of BBB alterations subsequent to H/R using a functionally intact model (i.e., in vivo) offers additional insight. Additionally, in vivo BBB examinations take into account the interactions of other cell types (i.e., glial and neuronal), blood flow dynamics and supply (i.e., shear stress, nutrient delivery, waste removal), and various peripheral influences, all of which can contribute to the cerebral microvascular stress response. Therefore, whole animal modeling can provide insight into the pathophysiology associated with cerebral H/R and BBB alteration, which may not be fully evaluated in vitro.

Using a commercially available $O_2$-controlled hypoxic chamber (normobaric) as a reproducible method of $O_2$ deprivation, we evaluated alterations in the in vivo rat BBB on reoxygenation after hypoxia. This approach confers an acute moderate to severe hypoxic insult that has been used previously to examine the effects of $O_2$ deprivation in the CNS (5, 31, 32). Additionally, this model does not limit blood flow, which thereby eliminates reperfusion-associated shear-stress variables. With this approach, evaluation of blood chemistries ($P_{O_2}$, $P_{CO_2}$, electrolyte concentrations, etc.) over the course of examination can be sampled, which provides a measure of the hypoxic insult on the CNS microvasculature. Additionally, this method of analysis allows for assessment of in vivo BBB alterations with relatively low trauma and thereby allows examination of a dynamically altered BBB without extensive damage to the microvasculature.

Recent research has provided significant insight into the molecular aspects of BBB TJs (35, 67), yet little is known concerning tight junctional regulation under physiological and pathological conditions. Our investigation provides mechanistic insight into the physiological and pathological changes associated with hypoxia and the in vivo cerebral microvasculature. This study focuses on BBB integrity when the animal is initially reoxygenated to evaluate tight junctional alterations after a hypoxic insult. Owing to differences in experimental conditions (i.e., degree and duration of hypoxia, type of anesthetic, etc.) that are apparent in the literature, we evaluated several model conditions [blood pressure (BP), blood gas chemistries, cerebral blood flow (CBF), and brain ATP concentrations] to establish a consistent level of insult and resultant effect while examining functional and molecular changes in the BBB.

## METHODS

*Radioisotopes, antibodies, and chemicals.* The [$^{14}$C]sucrose (0.44 Ci/mmol) was purchased from NEN Research Products (Boston, MA), and [$^3$H]butanol (5 Ci/mmol) was purchased from American Radiolabeled Chemicals (St. Louis, MO). TS-2 tissue solublizer and Budget Solve liquid scintillation cocktail were purchased from Research Products International (Mt. Prospect, IL). Unless otherwise specified, all other chemicals and reagents were purchased from Sigma (St. Louis, MO).

Anti-ZO-1, anti-occludin, and anti-claudin-3 antibodies (documented to react with rat) were purchased from Zymed Laboratories (San Francisco, CA). Anti-ZO-1 (0.5 mg/ml) is a monoclonal mouse antibody specific for the ZO-1 protein (220 kDa) directed against amino acids 334–634 of human ZO-1 cDNA. Anti-occludin (0.5 mg/ml) is a monoclonal mouse antibody specific for the occludin protein (65 kDa) directed against the COOH-terminal 150 amino acids of human occludin. Anti-claudin-3 (0.25 mg/ml) is a polyclonal rabbit antibody that recognizes the COOH-terminal region of the protein (22 kDa). Anti-actin (0.2 mg/ml) mouse monoclonal antibody (Sigma) is directed against the COOH terminus of the actin protein (42 kDa; clone AC-40) and is reported to react with rat actin. Anti-mouse IgG and anti-rabbit IgG horseradish peroxidase-conjugated secondary antibodies were purchased from Amersham (Buckinghamshire, UK).

*Hypoxic treatment.* Experimental protocols were approved by the Institutional Animal Care and Use Committee at the University of Arizona. Female adult Sprague-Dawley rats (Harlan; Indianapolis, IN) weighing 250–300 g were used for all experiments. Rats were housed under standard 12:12-h light-dark conditions and received food ad libitum.

Rats underwent a hypoxic insult (6, 10, 14, and 18% $O_2$ for 1 h or 6% $O_2$ for 30 min) in an $O_2$-controlled hypoxic chamber (Coy Laboratory Products; Grass Lake, MI) while under anesthesia with subsequent reoxygenation to room air (21% $O_2$). This was performed to identify an insult that would result in a significant permeability of the BBB as determined by in situ brain perfusion of [$^{14}$C]sucrose. Controls consisted of rats maintained over an identical time course in room air (21% $O_2$). Rats received 1.0 ml/kg im of anesthetic cocktail (in mg/ml: 78.3 ketamine, 3.1 xylazine, and 0.6 acepromazine). All procedures were performed while the rats were under anesthesia for purposes of consistency across analyses. Body temperature was maintained at 37°C with a heating pad (Harvard Apparatus; Holliston, MA).

*In situ brain perfusion.* The in situ brain-perfusion method was used to establish an appropriate hypoxic insult that would result in an alteration of BBB permeability. This procedure also maintains a constant cerebral flow of perfusion medium and thereby eliminates peripheral blood flow variables and hydrostatic changes that might occur while BBB integrity is determined. After hypoxic insult (6, 10, 14, and 18% $O_2$ for 1 h and 6% $O_2$ for 30 min) and 10 min of reoxygenation (21% $O_2$), a paracellular permeability marker, [$^{14}$C]sucrose (mol wt 342), was perfused. Multiple-time uptakes (5, 10, and 20 min) were measured after 6% $O_2$ exposure for 1 h and reoxygenation for 10 min.

Rats ($n = 4$) were removed from the hypoxic chamber while in an anesthetized state and were heparinized (10,000 U/kg).

The carotid arteries were cannulated with silicone tubing, and the jugular veins were cut. The time interval for removal from the hypoxic chamber to the start of perfusion was 10 min; during this time, respiration rate was stabilized. The perfusion medium (50) consisted of Evans blue dye in a mammalian Ringer solution [117.0 mM NaCl, 4.7 mM KCl, 0.8 mM $MgSO_4 \cdot H_2O$, 24.88 mM $NaHCO_3$, 1.2 mM $KH_2PO_4$, 2.5 mM $CaCl_2 \cdot 6H_2O$, 10 mM D-glucose, 39 g/l dextran (mol wt 70,000), and 1 g/l BSA], which was oxygenated with 95% $O_2$-5% $CO_2$. Ringer solution was then pumped through a heating coil (37°C), filtered, and debubbled before it entered the animal. The paracellular permeability marker [14C]sucrose was infused (1.5 ml/min) into the inflow of the perfusate using a slow-drive syringe pump (model 22, Harvard Apparatus) for 10 min. After a set perfusion time, the rat was decapitated, the brain was removed, and the choroid plexuses were excised. The brain was then segmented and placed in weighed vials. The perfusate containing the radiolabeled compounds was collected from each respective carotid cannula at the termination of perfusion to serve as a reference.

Brain samples were treated in a uniform manner with 1 ml of tissue solubilizer (TS-2, Research Products International; Mount Pleasant, IL) added to each respective sample. After solubilization, 100 μl of 30% glacial acetic acid was added to the samples to eliminate chemiluminescence. Budget Solve liquid scintillation cocktail (4 ml, Research Products International) was added, and samples were measured for radioactivity (LS 5000 TD counter, Beckman Instruments; Fullerton, CA). The [14C]sucrose activities were converted from counts per minute to disintegrations per minute with the use of internal stored quench curves.

*Capillary depletion.* Capillary depletion analysis ($n = 6$ rats) was performed to assure that measured [14C]sucrose was not increased via trapping within the endothelial cells of the microvasculature (61). This procedure was performed on control and 6% $O_2$ for 1 h-treated (with 10-min reoxygenation) groups, as the rats undergoing 6% $O_2$ for 1 h were the only group to show statistically significant permeability as shown by in situ brain perfusion. Briefly, after a 10-min in situ brain perfusion, the brain was removed and the choroid plexuses were excised. Brain tissue (~500 mg) was homogenized in 1.5 ml of capillary depletion buffer (in mM: 10 HEPES, 141 NaCl, 4 KCl, 2.8 $CaCl_2$, 1 $MgSO_4$, 1 $NaH_2PO_4$, and 10 D-glucose, pH 7.4) kept on ice. Ice-cold 26% dextran (2 ml; mol wt 60,000) was added, and homogenization was repeated. Tissue homogenization with vortexing serves to remove residual perfusion Ringer solution from the capillaries. Aliquots of homogenate were centrifuged at 5,400 $g$ for 15 min (Beckman Instruments; Fullerton, CA), and supernatant was separated from the vascular pellet. Homogenization procedures were performed within 2 min of the animal's death. The homogenate, supernatant, and pellet were taken for radioactive counting after solubilization as described previously.

*Calculation of in situ brain perfusion and capillary depletion.* The brain concentration of [14C]sucrose from in situ brain perfusion and in situ brain perfusion with capillary depletion (brain homogenate, supernatant, and pellet) analysis was expressed as the percent ratio ($R_{brain}$, in %) of tissue ($C_{brain}$, in disintegrations·min$^{-1}$·g$^{-1}$ of disintegrations· min$^{-1}$·ml$^{-1}$) to perfusate activities ($C_{perfusate}$, in disintegrations·min$^{-1}$·ml$^{-1}$): $R_{brain} = (C_{brain}/C_{perfusate}) \times 100$.

*Expression of results for multiple-time uptakes.* The equation for multiple-time point uptake was used (47) as

$$C_{brain}/C_{perfusate} = K_{in} \times \left[ \left( \int_0^t C_{perfusate}(t)dt \right) \Big/ C_{perfusate} + V_i \right]$$

where $C_{brain}$ is the amount of test solute per unit mass of brain at time $t$, and $C_{perfusate}$ is the perfusion fluid concentration of test solute at time $t$. The value for $C_{perfusate}$ remained constant during these experiments, and a plot of $C_{brain}/C_{perfusate}$ against time produces a straight line with slope $K_{in}$ (the initial unidirectional transfer constant) and an ordinate intercept of $V_i$ (the initial volume of distribution).

*[3H]butanol CBF analysis.* The [3H]butanol method for CBF was used to determine whether CBF was altered over the course of in situ brain perfusion, as significant alterations in flow may result in a paracellular permeability change (1). The perfusion methods of Preston et al. (50) and Zlokovic et al. (72) were adapted to determine both CBF and rate of cerebral perfusion in situ. This procedure was performed on control and 6% $O_2$ for 1 h-treated (with 10-min reoxygenation) groups, as the rats undergoing 6% $O_2$ for 1 h were the only group to show statistically significant permeability by in situ brain perfusion. The rates of both CBF and cerebral perfusion (in situ) were calculated using the equations for [3H]butanol uptake (18). In situ brain perfusion was carried out using an isotope-free Ringer solution that contained 4 ml/l of unlabeled 100% ethanol to saturate endogenous alcohol dehydrogenase, and the operation was performed as described for 10 min with no radioactive isotope ($n = 4$ rats). The [3H]butanol (1 μCi/μl) was added via a slow-drive syringe pump for the last 10 s before decapitation. The brain was weighed, and samples of both brain and perfusion medium were taken for radioactivity measurement.

*Calculating CBF.* CBF was calculated using the equation (18)

$$F_{bl} = -\lambda_{br} \ln[(1 - C_{brain(t)}/\lambda_{br} \times C_{a(t)})/t] \text{ ml/g}$$

where $F_{bl}$ is the flow rate (in ml/min) per unit mass ($g^{-1}$), $C_a$ is the [3H]butanol concentration in arterial inflow at time $t$, $C_{brain}$ is the radioactivity in brain at time $t$, and $\lambda_{br}$ is the distribution ratio of [3H]butanol between the brain and the perfusate at steady state. Extraction of the tracer from the blood is assumed to be complete during a single capillary pass.

The distribution ratio $\lambda_{br}$ was determined using a control group perfused with a constant [3H]butanol concentration for 10 min. The value of $\lambda_{br}$ was calculated as a ratio of [3H]butanol radioactivity in the brain vs. radioactivity found in the arterial inflow (perfusate) at steady state. Values of $\lambda_{br}$ are representative of the total distribution of [3H]butanol in the brain following a 10-min perfusion after treatment (6% $O_2$ for 1 h hypoxia with 10-min reoxygenation) and control. The value of $\lambda_{br}$ was estimated from data for a single bolus passage of [3H]butanol and is in agreement with the assumption that brain uptake of [3H]butanol is limited by perfusion flow determined directly by equilibration between brain and perfusate.

*Laser Doppler CBF examination.* CBF was monitored on the surface of the cerebral cortex of both the right ($n = 8$) and left ($n = 9$) parietal cortices via laser Doppler flowmetry (MBF3D, Moor Instruments; Wilmington, DE) to provide an assessment of real-time cortical tissue blood flow before, during, and after hypoxic insult (6% $O_2$ for 1 h). The Moor laser Doppler uses laser radiation generated by a semiconductor laser diode (wavelength, ~780 nm; maximum accessible power, 1.6 mW). Animals were placed in the prone position, and the head was firmly immobilized in a stereotaxic frame (Stoelting; Wood Dale, IL). A burr hole (~2 mm in diameter) was drilled 5 mm lateral and 1 mm posterior to the bregma. The laser Doppler probe (MP3, 30 mm) was positioned directly on the right or left parietal cortex for continuous measurement of local cortical blood flow from before the

onset (baseline) of hypoxic insult until ~1 h after insult (reoxygenation). Measurement of flux during and after insult was normalized to initial baseline values for each animal. Flux takes into account the product of the average speed and concentration of moving red blood cells in the tissue-sample volume (65).

*BP measurement.* Mean arterial BP was measured to assess blood flow changes throughout insult via cannulation of the right carotid artery of the anesthetized rats ($n = 4$) over a course of hypoxia (6% $O_2$ for 1 h) and subsequent reoxygenation; the BP-1 pressure monitor and the Duo 18 chart recorder (WPI; Sarasota, FL) were used. The cannula was flushed with heparin before insertion and was sutured in place over the course of analysis. Results were normalized against initial normoxic BP readings for each respective rat.

*Blood gas and electrolyte analysis.* Blood gas and electrolyte analyses were conducted to validate the degree of hypoxic insult at 6% $O_2$ compared with normoxic levels ($n = 3$ rats) and to account for circulatory alterations. Measurements of $P_{O_2}$, $P_{CO_2}$, $HCO_3^-$ concentration, $O_2$ saturation, ion concentration ($Na^+$, $K^+$, $Ca^{2+}$), and pH were performed throughout the 1-h hypoxic exposure and up to 2 h posthypoxic reoxygenation using the ABL 505 (Radiometer; Copenhagen, Denmark). Blood was taken from the femoral artery (~100-μl aliquots) via a heparinized syringe and was immediately analyzed. Blood volume was maintained with equal injections of 0.9% saline to avoid hypovolemia.

*Gross brain water weight.* Gross brain water weight was used to assess edema in anesthetized rats. Brains of control, hypoxic (6% $O_2$ for 1 h, with brain removed within the hypoxic chamber), and posthypoxic-treated (10-min reoxygenation) groups were extracted ($n = 4$ rats), divided into hemispheres, weighed, and dried (75°C) in an oven (48 h). Final dry brain weights were confirmed after three consistent measurements at the same weight and were reported as percent ratios of wet weights.

*Whole brain ATP measurement.* ATP levels were measured in whole brain homogenate for control, hypoxic (6% $O_2$ for 1 h, with brain removed within the hypoxic chamber), and posthypoxic (10-min reoxygenation)-treated animals ($n = 5$) to assess any potential alterations in gross brain metabolism. A chemiluminescent method that uses luciferin-luciferase was employed to determine ATP concentrations. Rats were decapitated after treatment or control, and each hemisphere (cerebral cortex) was removed, weighed, and homogenized in 10 ml of 0.1 M NaOH (to inactivate cellular ATPase activity) at 4°C with a glass mortar and Teflon pestle for 20 strokes until tissue was homogenous. ATP was extracted from the tissue within 1 min after the brain was removed. Samples were assayed using the ATPLite-M luminescent ATP detection assay kit (Packard BioScience; Meriden, CT), and chemiluminescence was measured using the GENios microplate luminometer (Tecan; Research Triangle Park, NC). ATP concentrations were calculated from a standard curve and were normalized against wet-tissue weights in grams (expressed as μmol/g).

*Microvessel isolation.* After hypoxic treatment (6% $O_2$ for 1 h, with 10-min reoxygenation) or control, anesthetized rats were decapitated and brains were removed ($n = 4$). Meninges and choroid plexuses were excised, and the cerebral hemispheres were homogenized in 4 ml of microvessel isolation buffer [103 mM NaCl, 4.7 mM KCl, 2.5 mM CaCl$_2$, 1.2 mM KH$_2$PO$_4$, 1.2 mM MgSO$_4$, 15 mM HEPES, 2.5 mM NaHCO$_3$, 10 mM D-glucose, 1 mM sodium pyruvate, 10 g/l dextran (mol wt 64,000), pH 7.4]. Ice-cold 26% dextran (4 ml) was added to the homogenates, which were then vortexed and centrifuged at 5,600 $g$ for 10 min before supernatant aspiration. Pellets

were resuspended in 10 ml of microvessel isolation buffer and passed through a 100-μm filter (Falcon, Becton Dickinson; Franklin, NJ). The filtered homogenates were centrifuged at 3,000 $g$, and protein was extracted from the pellets using 6 M urea lysis buffer (6 M urea, 0.1% Triton X-100, 10 mM Tris, pH 8.0, 1 mM dithiothreitol, 5 mM MgCl$_2$, 5 mM EGTA, and 150 mM NaCl) with EDTA-free protease inhibitor cocktail (Roche; Mannheim, Germany). Protein concentrations were determined by bicinchoninic acid protein assay (Pierce; Rockford, IL) with BSA as a standard.

*Western blot protein analysis.* Microvessel isolates were analyzed for protein expression of occludin, ZO-1, claudin-3, and actin using Western blot ($n = 4$ rats). Samples (30 μg) were separated using an electrophoretic field on Novex Trisglycine gels (10% gel for occludin analysis; 4–12% gel for all other proteins) at 125 V for 75–90 min. GelCode Blue Stain (Pierce) was used to normalize protein loading. The proteins were transferred to polyvinylidene fluoride membranes with 240 mA at 4°C for 30 min. The membranes were blocked using 5% nonfat milk-Tris-buffered saline (20 mM Tris base, 137 mM NaCl, pH 7.6) with 0.1% Tween 20 for 4 h and were then incubated overnight at 4°C with primary antibodies (1:1,000–1:2,000 dilution) in PBS-0.5% BSA. The membranes were washed with 5% nonfat milk-Tris-buffered saline buffer before incubation with the respective secondary antibody at a 1:2,000 dilution (in PBS-0.5% BSA) for 30 min at room temperature. Blots were developed using the enhanced chemiluminescence method (ECL$^+$; Amersham Life Science Products; Springfield, IL), and protein bands were visualized on X-ray film. Semiquantitation of the protein was done with the use of Scion image software (Scion; Frederick, MD), and the results are reported as percentages of controls.

*Statistical analysis.* For all experiments, data are presented as means ± SE. All parameters were compared by ANOVA followed by post hoc Newman-Keuls analysis where appropriate. Statistical significance is indicated as $P < 0.05$ or $P < 0.01$ unless otherwise stated.

## RESULTS

*In situ brain perfusion.* In situ perfusion was performed after 10 min of posthypoxic reoxygenation. Rat respiration rates were assessed to assure stability before the procedure was initiated. Paracellular permeability was analyzed with the use of [$^{14}$C]sucrose as a marker. Figure 1 shows the ratio percentage of brain uptake of the marker. No increase in permeability was observed following 10, 14, and 18% $O_2$ for 1 h or 6% $O_2$ for 30 min of hypoxic insult with 10 min of reoxygenation. However, an insult of 6% $O_2$ for 1 h with subsequent 10-min reoxygenation showed a 32% increase ($P < 0.05$) over control.

Multiple-time uptake study (Fig. 2) shows a significantly higher rate of brain uptake for H/R (6% $O_2$ for 1 h followed by 10-min reoxygenation) rats compared with controls ($K_{in}$ values of 0.89 ± 0.03 vs. 0.07 ± 0.1 μl·min$^{-1}$·g$^{-1}$, respectively; $P < 0.01$). Initial volumes of distribution ($V_i$; intercepts of linear regression) were not significantly different from one another (14.6 compared with 12.0 μl/g, respectively), which indicates no change in vascular volume.

*Capillary depletion.* Measurements of capillary depletion (Fig. 3) showed no difference in the ratio of uptake in the pellet (i.e., vascular component) portion between control and treated (6% $O_2$ for 1 h followed by
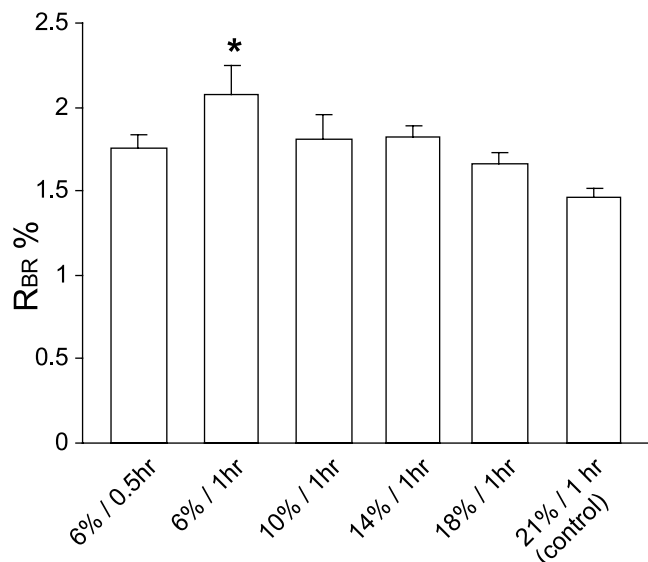
Fig. 1. Blood-brain barrier (BBB) paracellular permeability in post-hypoxic rat (10-min reoxygenation after hypoxic treatment): hypoxia at 6, 10, 14, and 18% $O_2$ for 1 h and 6% $O_2$ for 0.5 h. Data are expressed as percent ratio of tissue to perfusate [$^{14}$C]sucrose ($R_{Br}$, in %). Perfusion time was 10 min, and values are means $\pm$ SE ($n = 4$ rats). Statistical significance was determined using one-way ANOVA followed by Newman-Keuls post hoc test; *$P < 0.05$, significant difference compared with control (normoxic, 21% $O_2$).
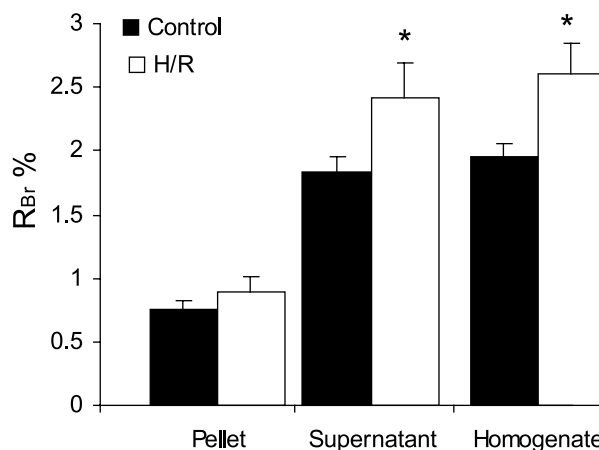


Fig. 3. BBB paracellular permeability in posthypoxic rat (10-min reoxygenation after hypoxic treatment, H/R); hypoxia treatment was 6% $O_2$ for 1 h. Data are expressed as a percent ratio of tissue to perfusate [$^{14}$C]sucrose ($R_{Br}$, in %) within the pellet (i.e., vascular fraction), supernatant (i.e., nonvascular fraction), and homogenate (i.e., total brain). Perfusion time was 10 min. Values are means $\pm$ SE ($n = 6$ rats); *$P < 0.05$, significant difference compared with control (normoxic, 21% $O_2$).

10-min reoxygenation) rats. With respect to each group (control or posthypoxic), the portion associated with brain parenchyma (i.e., supernatant) showed an increase ($P < 0.05$) in the posthypoxic reoxygenation. The homogenate portion showed an increase ($P < 0.05$) in the posthypoxic reoxygenated sample compared with control that was equivalent to the ratio seen in Fig. 1. There was not a statistically significant interaction between treatments (control and posthypoxic reoxygenated) vs. the respective vascular portions (homogenate, supernatant, and pellet) as determined by two-way ANOVA ($P = 0.275$).

*[$^3$H]butanol CBF analysis.* To assess whether the increase in brain uptake on initial reoxygenation (10 min posthypoxia, 6% $O_2$ for 1 h) was attributable to increased CBF during the in situ brain perfusion procedure, the [$^3$H]butanol method of CBF analysis was performed under identical conditions as the in situ brain perfusion. CBF ($F_{br}$), measured after a 10-min in situ perfusion, was calculated at $t = 10$ s. Values were $C_{brain(t)}$: control, $0.02 \pm 0.0061$ $\mu$Ci/g and H/R, $0.04 \pm 0.0095$ $\mu$Ci/g; $C_a$: control, $68.3 \pm 5.35$ nCi/g and H/R, $55.1 \pm 2.85$ nCi/g; and $\lambda_{br}$: control, $0.64 \pm 0.04$ and H/R, $0.58 \pm 0.09$. The CBF values were $1.28 \pm 0.043$ (control) vs. $0.995 \pm 0.024$ ml·min$^{-1}$·g$^{-1}$ (H/R), with CBF ranges of $1.19-1.39$ (control) and $0.97-1.07$ (H/R). The results show a decrease ($P < 0.01$) in CBF in the H/R group compared with control over the course of the perfusion while remaining within established physiological range ($0.8-1.49$ ml·min$^{-1}$·g$^{-1}$; Refs. 18, 54).

*Laser Doppler CBF examination.* The average CBF (flux) increased ($39 \pm 8.3\%$) in both the right and left parietal cortices as normalized to baseline measure-
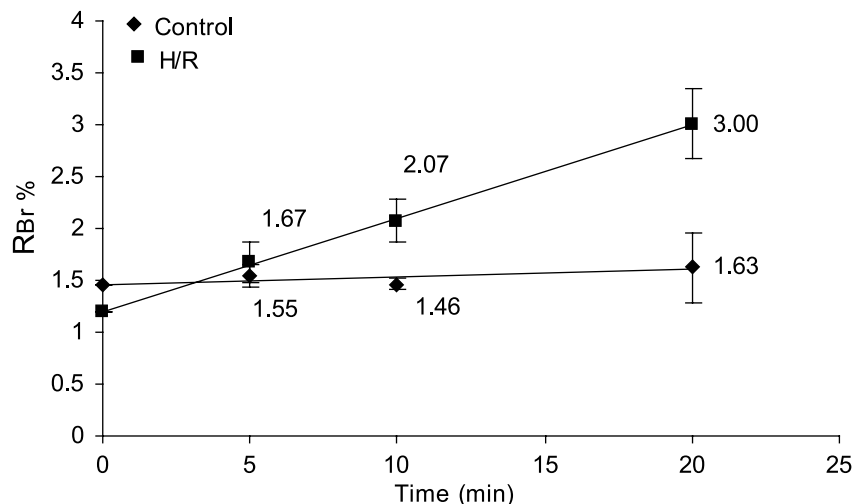


Fig. 2. Multiple-time uptake analysis of BBB paracellular transport, in situ brain perfusion, with control (normoxic, 21% $O_2$) and posthypoxic [10-min reoxygenation, hypoxia-reoxygenation (H/R)] treatment. Data are expressed as a percent ratio of tissue to perfusate radioactivites ($R_{Br}$, in %) with use of [$^{14}$C]sucrose (control $K_{in}$, $0.07 \pm 0.1$; H/R $K_{in}$, $0.89 \pm 0.03$ $\mu$l·min$^{-1}$·g$^{-1}$; $P < 0.01$). Perfusion times were 5, 10, and, 20 min; values are means $\pm$ SE ($n = 4$ rats).

Fig. 4. Representative measurement of real-time laser Doppler cerebral blood flow (CBF; flux) observed over the course of hypoxia (6% $O_2$ for 1 h) and subsequent reoxygenation (with room air; 21% $O_2$). 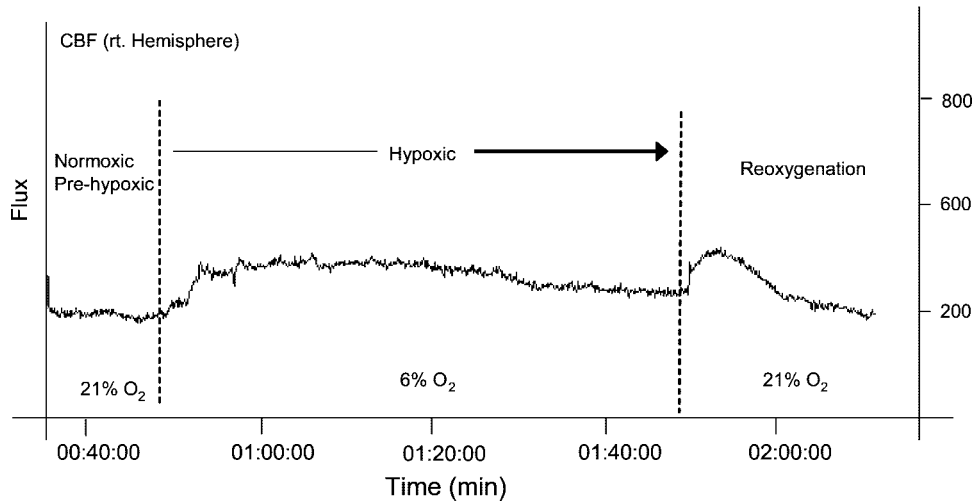Flux takes into account the product of the average speed and concentration of moving red blood cells in the tissue sample volume.

ments over 1 h of hypoxic insult. The average increase in CBF recorded shows both an initial rise and a subsequent decline (Fig. 4) over the 1-h hypoxic stress, which corresponds to the rise and fall in BP (Fig. 5). The averaged maximum peak increase over normalized baseline levels was 2.7-fold, and this occurred within the first 5–10 min of hypoxic exposure (averaged range, 267 $\pm$ 20% above to 43 $\pm$ 2.6% below normalized baseline). Upon reoxygenation (with 21% $O_2$), a second increase in CBF was observed (17 $\pm$ 6.2%) that also corresponded to BP change. Baseline levels were reached after 10–15 min of reoxygenation (averaged range, 278 $\pm$ 54% above to 44 $\pm$ 4.4% below normalized baseline).

*BP measurement.* Analysis reveals a moderate drop in BP with initial onset of hypoxic treatment (6% $O_2$ for 1 h) with subsequent reestablishment in BP. Hyperventilation rate corresponded to maintenance of BP with a gradual shift to a deep (hyperpnea) rate of respiration that corresponded to the decline in BP. Hypoxia resulted in a marked hypotension, hypocapnia, and alkalosis. Reoxygenation (room air, 21% $O_2$) resulted in an immediate increase in BP associated

with an increase in the hyperventilatory response for a period of ~10 min. The percent average decline in BP (in mmHg) over hypoxic insult (averaged maximum to averaged minimum) was ~40% with an ~45% increase upon reoxygenation (over hypoxic minimum) and subsequent normalization of BP within ~10 min of reoxygenation.

*Blood gas and electrolyte analysis.* Blood gas analysis showed a classic acute/subacute respiratory response resulting from hypoxia. Table 1 shows a rapid increase in pH during the initial hypoxic insult (from 7.35 to 7.52) and compensation by the end of the 1-h hypoxia with normalization to baseline readings after 10 min of reoxygenation. Partial pressure readings of $O_2$ (in mmHg) indicate an ~73% decrease throughout the course of the hypoxic insult with a recovery in $P_{O_2}$ to baseline within the initial 10-min reoxygenation. $P_{CO_2}$ readings (in mmHg) indicate an ~61% decrease over the course of the hypoxic insult with a recovery to baseline levels by 90 min of reoxygenation. $HCO_3^-$ concentration (in mmol/l) decreased ~46% over the course of the hypoxic insult with recovery to baseline levels by 120 min of reoxygenation. $Na^+$ (meq/l) con-
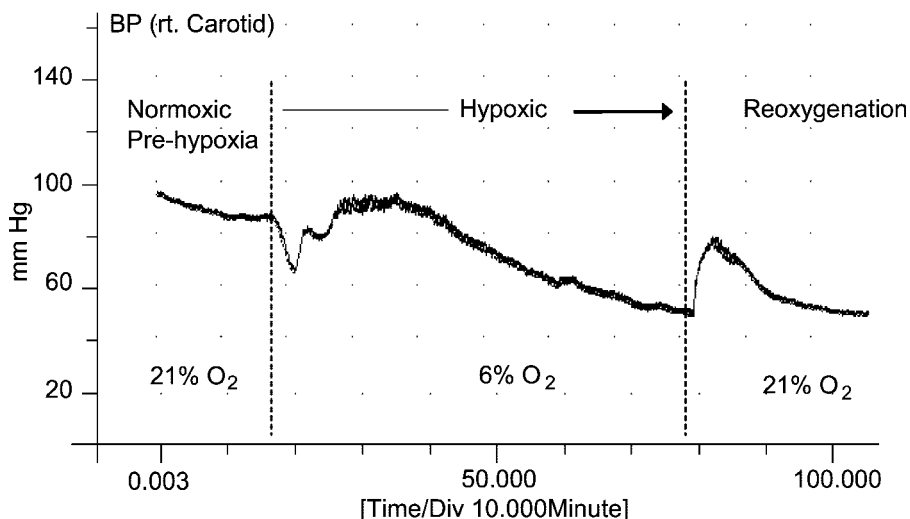


Fig. 5. Representative measurements (in mmHg) of mean arterial blood pressure (BP) observed over the course of hypoxia (6% $O_2$ for 1 h) and subsequent reoxygenation (room air, 21% $O_2$) via cannulation of the right carotid artery.

Table 1. *Blood gas and electrolyte measurements during hypoxia-reoxygenation treatment*

| Time Course and Treatment | pH | $P_{CO_2}$, mmHg | $P_{O_2}$, mmHg | $HCO_3^-$, mmol/l | $O_2$ Saturation, % | $K^+$, meq/l | $Na^+$, meq/l | $Ca^{2+}$, meq/l |
|---|---|---|---|---|---|---|---|---|
| Pretreatment | $7.35 \pm 0.02$ | $46.6 \pm 7.4$ | $101.6 \pm 9.0$ | $24.8 \pm 3.0$ | $97.1 \pm 0.9$ | $3.27 \pm 0.35$ | $142 \pm 1.5$ | $2.17 \pm 0.41$ |
| Hypoxia, min | | | | | | | | |
| 10 | $7.52 \pm 0.01^*$ | $19.3 \pm 3.3^*$ | $29.3 \pm 5.0$† | $15.6 \pm 2.7^*$ | $62.9 \pm 9.7$† | $3.40 \pm 0.35$ | $140 \pm 2.0$ | $1.61 \pm 0.18$ |
| 20 | $7.51 \pm 0.01^*$ | $20.8 \pm 2.5^*$ | $25.9 \pm 3.1$† | $16.5 \pm 1.7^*$ | $56.4 \pm 7.5$† | $3.83 \pm 0.50$ | $137 \pm 2.3$ | $2.09 \pm 0.14$ |
| 30 | $7.49 \pm 0.01^*$ | $18.7 \pm 1.8^*$ | $27.2 \pm 3.6$† | $14.1 \pm 1.3$† | $58.2 \pm 8.0$† | $3.77 \pm 0.50$ | $136 \pm 3.5$ | $2.08 \pm 0.31$ |
| 40 | $7.47 \pm 0.01^*$ | $17.7 \pm 1.7^*$ | $27.7 \pm 3.2$† | $12.6 \pm 0.9$† | $58.5 \pm 7.5$† | $4.20 \pm 0.53$ | $135 \pm 2.6$ | $2.18 \pm 0.17$ |
| 50 | $7.46 \pm 0.01$ | $16.9 \pm 1.9^*$ | $27.5 \pm 3.7$† | $11.8 \pm 1.1^*$ | $57.2 \pm 8.7$† | $4.77 \pm 0.42$ | $131 \pm 0.9^*$ | $2.49 \pm 0.10$ |
| 60 | $7.43 \pm 0.03$ | $16.1 \pm 1.1^*$ | $28.8 \pm 5.5$† | $10.6 \pm 1.4$† | $56.8 \pm 11.5$† | $4.83 \pm 0.32$ | $132 \pm 0.6^*$ | $2.51 \pm 0.12$ |
| Reoxygenation, min | | | | | | | | |
| 10 | $7.3 \pm 0.02$ | $22.6 \pm 3.0^*$ | $104.2 \pm 20.4$ | $10.7 \pm 1.6$† | $96.2 \pm 2.0$ | $3.60 \pm 0.38$ | $138 \pm 1.5$ | $1.68 \pm 0.29$ |
| 30 | $7.36 \pm 0.04$ | $31.3 \pm 3.5$ | $101.9 \pm 19.3$ | $17.3 \pm 2.8^*$ | $96.9 \pm 1.1$ | $3.50 \pm 0.78$ | $134 \pm 1.5$ | $2.37 \pm 0.20$ |
| 60 | $7.36 \pm 0.05$ | $33.1 \pm 2.6$ | $95.0 \pm 24.1$ | $18.9 \pm 3.1$ | $95.4 \pm 2.2$ | $4.03 \pm 0.45$ | $135 \pm 0.9$ | $2.44 \pm 0.11$ |
| 90 | $7.36 \pm 0.04$ | $34.6 \pm 4.6$ | $109.1 \pm 16.8$ | $18.8 \pm 1.7$ | $97.4 \pm 0.5$ | $4.43 \pm 0.95$ | $134 \pm 2.1$ | $2.37 \pm 0.34$ |
| 120 | $7.35 \pm 0.05$ | $36.1 \pm 4.1$ | $97.3 \pm 20.6$ | $20.5 \pm 1.8$ | $96.5 \pm 1.8$ | $4.15 \pm 0.37$ | $134 \pm 2.5$ | $2.61 \pm 0.16$ |

Values are means $\pm$ SE; $n = 3$ rats. Hypoxia (6% $O_2$) for 1 h with 2 h reoxygenation. Fluid replacement with 0.9% saline solution was performed to negate hypovolemia. Nonhypoxic controls ($n = 3$ rats) on an identical time course exhibited no differences in values as pretreatment group. One-way repeated-measures ANOVA conducted for each parameter followed by Newman-Keuls post hoc test when appropriate. $^*P < 0.05$; †$P < 0.001$.

centration decreased ~7% by the end of the hypoxic insult with recovery to baseline levels by 10 min of reoxygenation. $Ca^{2+}$ and $K^+$ (meq/l) showed no statistically significant changes over the course of H/R.

*Gross brain weight measurements.* Averaged percent ratios of wet weights of brains were measured, which showed an increase ($P < 0.05$) from control ($78.4 \pm 0.37\%$) to a posthypoxic (10-min reoxygenation) weight of $79.4 \pm 0.21\%$. The increase did not reach statistical significance between hypoxic $79.0 \pm 0.14\%$ (6% $O_2$ for 1 h, with brain removed within the hypoxic chamber) and control brain weights.

*Whole brain ATP measurements.* The change in ATP brain levels between control ($2.10 \pm 0.11$ μmol/g) and hypoxic (6% $O_2$ for 1 h, brain removed within the hypoxic chamber)-treated animals ($2.69 \pm 0.49$ μmol/g) did not show a statistically significant alteration; however, the increase in ATP concentration did reach significance ($P < 0.05$) on reoxygenation: the value for control vs. posthypoxic treatment (10-min reoxygenation) was $2.91 \pm 0.14$ μmol/g. Brain ATP concentration was consistent with that previously shown in the literature (11).

*Western blot analysis.* Western blot analyses demonstrated alterations in expression of tight junctional proteins after H/R (6% $O_2$ for 1 h with 10-min reoxygenation). Figure 6*A* shows the integral protein occludin with dual bands at 65 and 63 kDa. The 65-kDa band (β-band) shows no significant change, whereas the 63-kDa band (α-band) shows a significant ($P < 0.01$) decrease ($42.1 \pm 10.1\%$) in H/R compared with control. Figure 6*B* shows no significant difference in ZO-1 expression after H/R compared with control. Figure 6*C* shows no significant difference in claudin-3 expression after H/R compared with control. Figure 6*D* shows no significant difference in actin expression after H/R compared with control.

## DISCUSSION

In this study, we examined BBB permeability during initial posthypoxic reoxygenation in an in vivo rat model to correlate previous in vitro and in vivo H/R studies and to further our understanding of tight junctional complex alterations. To examine the relationship of H/R stress on cerebral microvasculature, it was first necessary to establish an in vivo model of hypoxic insult sufficient to result in BBB permeability change during reoxygenation.

The effect of H/R on the in vivo BBB was assessed using in situ brain perfusion across a range of hypoxic conditions with [14C]sucrose as a permeability marker (see Fig. 1). The data show a significant increase in cerebral microvascular permeability after a posthypoxic insult (6% $O_2$ for 1 h) and an initial 10 min of reoxygenation. To ensure that increased BBB permeability was due to increased paracellular diffusion and not changes in vascular space or vascular trapping, capillary depletion and CBF analysis were performed in conjunction with the in situ procedure. Capillary depletion analysis (see Fig. 3) showed that the amount of [14C]sucrose within the vascular pellet was not different from control. Furthermore, the increase in [14C]sucrose associated with homogenate and supernatant, compared with the respective controls, would indicate impairment of the BBB. CBF was assessed over an identical course using the [3H]butanol method to assure that the observed permeability by in situ brain perfusion was not a result of flow variables. CBF values measured in control rats were consistent with previously reported values (18, 54, 70). Although our study actually showed a statistical decrease in CBF in the posthypoxic reoxygenation group (6% $O_2$ for 1 h), this decrease was well within the established normal physiological range (18, 54, 70). To further substantiate the observed increase in BBB permeability, a multiple-time uptake analysis was performed using the in
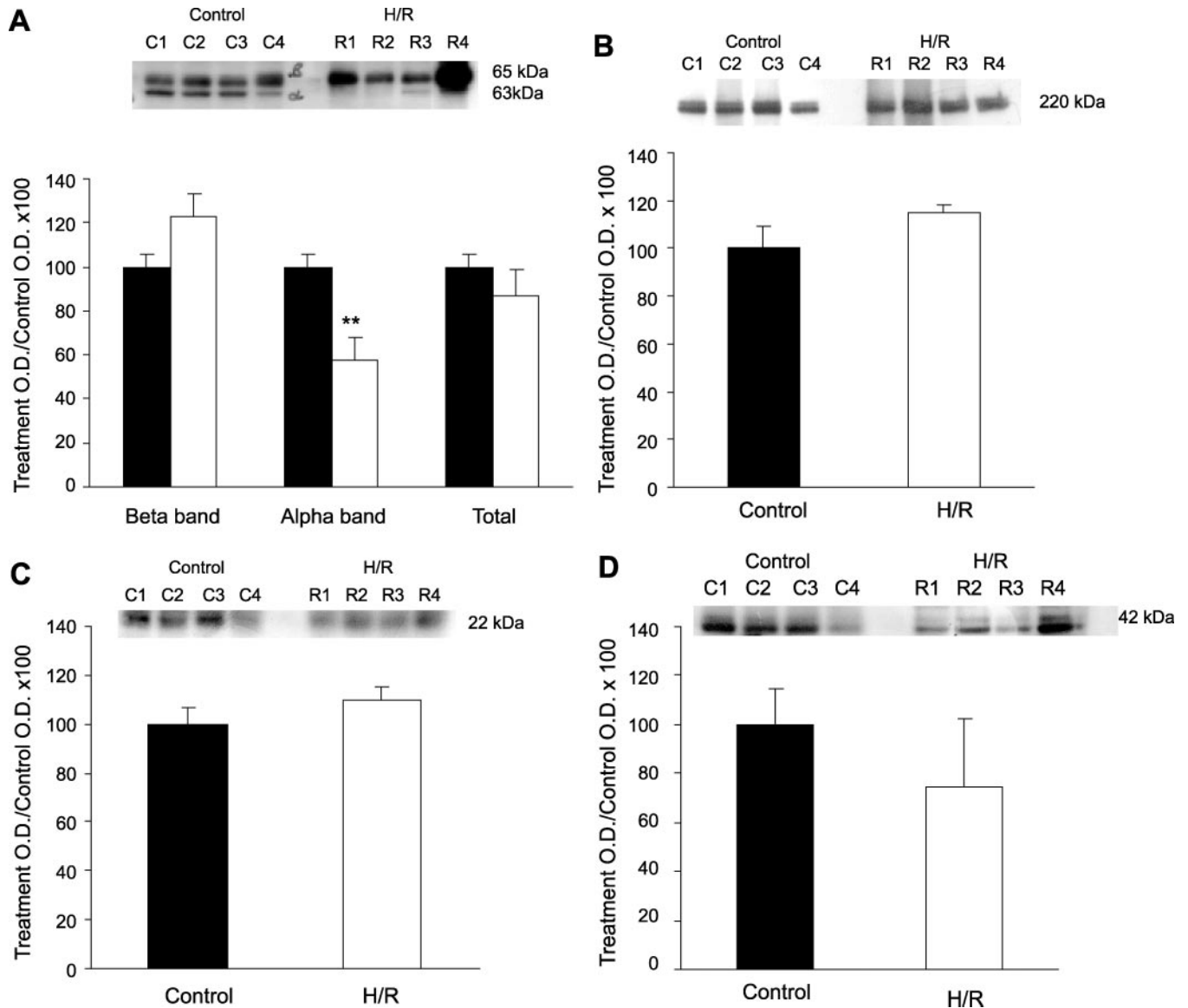
Fig. 6. Western blot analyses show expression of tight junctional proteins to be altered during posthypoxic reoxygenation (10-min reoxygenation after hypoxic treatment of 6% $O_2$ for 1 h; H/R). *A*: integral protein occludin shows as a dual band at 65 and 63 kDa, which is indicative of phosphorylated (β-band) and nonphosphorylated (α-band) states, respectively. There was a significant decrease in expression of the α-band on H/R. *B*: zonula occludens-1 expression after H/R was unchanged. *C*: claudin-3 expression after H/R was unchanged. *D*: actin expression after H/R was unchanged. **$P < 0.01$ vs. control; $n = 4$ rats. OD, optical density.

situ brain perfusion procedure (see Fig. 2). There was no difference in the [$^{14}$C]sucrose uptake observed across time points for the control animals; however, a significant uptake change was shown for the H/R animals. The $V_i$ values for the control and H/R groups were not significantly different, which also indicates no change in vascular volume. These studies clearly indicate that H/R (6% $O_2$ for 1 h with 10-min reoxygenation) produced significant BBB permeability changes via increased paracellular diffusion in the brain microvasculature.

Blood gas, pH, and electrolyte analyses demonstrated a significant effect of hypoxia (6% $O_2$ for 1 h) on peripheral blood chemistries (Table 1). $P_{O_2}$ is critical in determining the $O_2$ gradient between systemic capillary blood and tissue. In the case of acute hypoxemia associated with alkalosis and hypocapnia, there is a left-shift in the hemoglobin dissociation curve with an enhanced affinity of hemoglobin for $O_2$. The greater affinity hemoglobin has for $O_2$, the less $O_2$ is transferred to the tissue. The severity of 6% $O_2$ for 1 h was compensated over the course of the insult with a reduction in $HCO_3^-$ concentration and subsequent correction of pH toward baseline levels. Upon reoxygenation (room air, 21% $O_2$), blood gas $O_2$ and pH values normalized to baseline levels within 10 min, and $P_{CO_2}$ normalized by 30 min. Models of high-altitude hypoxia show similar effects on blood gas and pH (5, 46). Blood $Na^+$ concentration measurements showed a gradual

decrease over the course of the 6% $O_2$ for 1 h hypoxic exposure. The $Na^+$ decrease observed over the hypoxic insult may indicate tissue influx, which is associated with ischemic edema (53). Under normal physiological conditions, tissue influx of osmotically active solutes such as $Na^+$ is regulated in a zero net-solute shift. However, secondary to energy failure, active $Na^+$ export fails and thereby alters both vascular and inter- and intracellular concentrations.

Despite the fact that the brain is markedly sensitive to $O_2$ deficiency, many studies have shown that energy metabolism of the brain is well maintained even at severe degrees of hypoxia. This study shows that ATP levels of the whole brain were not significantly altered between control (normoxic) and hypoxic (6% $O_2$ for 1 h, with brain removed within hypoxic chamber) animals; yet an ATP increase becomes significant on 10-min posthypoxic reoxygenation. Brain tissue concentrations of ATP, ADP, and AMP have been previously shown to remain in the normal range even when $Po_2$ values are reduced to 20–25 mmHg (3, 20, 30). The increase in ATP concentration on reoxygenation observed within our study may be a rebound effect associated with both increased glucose transport to the brain (38, 64) and elevated cerebral glucose utilization (5, 60) as previously shown during hypoxic stress accompanied with the resurgence of oxidative processes. In addition to glycolysis and oxidative phosphorylation, two other mechanisms involved in the maintenance of ATP levels, the creatine phosphokinase and adenylate reactions, may also be involved in the increase in ATP on initial reoxygenation. The extent by which the BBB is directly affected under H/R stress, related to ATP concentration, has not been determined in vivo. The brain capillary endothelium is characterized by a greater density of mitochondria than that of peripheral capillaries (44, 45). This greater mitochondrial density is required to maintain the significant active transport mechanisms, electrochemical gradients, autoregulatory adjustments, and regulation of tight junctional complexes. As such, requirement of a constant ATP supply may make the BBB particularly susceptible to an acute hypoxic insult. In vitro analysis of BBB endothelial cells (49) shows ATP levels during an extensive anoxic insult (0% $O_2$ for 24 h) have a 25% decrease in ATP, which indicates a relatively resilient cell line in terms of energy maintenance. Whether the in vivo BBB, with a greater degree of metabolic demands placed on it from the periphery and the CNS compared with in vitro modeling, is able to maintain such resiliency under hypoxic stress has not been assessed.

The hypoxic insult to the brain itself would be reduced, compared with the periphery, as a result of cerebral autoregulatory and cardiopulmonary compensation. Curtailed $O_2$ supply elicits an increase in CBF as a principle compensatory mechanism. The cerebral circulation has been described as a high-pass filter (71) with ineffective modulation of pressure-induced changes in CBF at high frequencies (>0.20 Hz). During high-frequency periods, the biophysical properties of

cerebral circulation including conductance, cerebrovascular impedance, and inertia of the blood column predominate with changes in BP transmitted directly into changes in CBF (37). Cerebral autoregulation has been proposed to be impaired under hypoxia (22, 57, 59), which would result in the dependency of CBF on BP. Analysis of our model indicates an increase in CBF and BP during the initial phase (10–20 min) of hypoxic insult as well as during the initial period of reoxygenation. Our analyses also indicate an increase in gross brain weight (i.e., edema) resulting from H/R. Edema has been linked to increased risk of hemorrhage from damaged vessels and excess fluid accumulation in brain extracellular space (52). High capillary perfusion pressure ($P_{cap}$) has been suggested to produce vasogenic edema (36, 59). Brain edema associated with cerebral vasodilation and $P_{cap}$ was addressed in a series of experiments by Krasney (35). Krasney showed that CBF and $P_{cap}$ increased over the course of hypoxia associated with an increase in epidural pressure and extravasation of Evans blue dye thereby confirming BBB permeation. However, further experiments have indicated that brain edema resulting from large increases in hydrostatic $P_{cap}$ induced by inhaled $CO_2$ or infused nitroglycerin (pressures higher than those observed from hypoxia) was much less than that resulting from hypoxia. This indicates that increased capillary pressure is not the sole factor involved in hypoxic-associated BBB permeability (34), which is supported by our in situ brain perfusion analyses.

Western blot analyses were performed to determine the potential alteration in specific tight junctional proteins of the BBB. Although no significant changes in protein expressions of claudin-3 (Fig. 6C), ZO-1 (Fig. 6B), or actin (Fig. 6D) were observed on H/R, this does not exclude the potential of cellular relocalization. Immunofluorescent examination of the in vitro BBB during H/R showed alterations in ZO-1 and occludin protein localization on reoxygenation that correlated with increased paracellular permeability, whereas claudin-1 (with antibody cross-reactivity to claudin-3) did not show any change in protein expression or localization (40). Actin, the primary protein that forms the cytoskeletal structure, has shown increased expression and stress tangles on H/R in vitro (9, 40). A qualification exists in reference to claudin-3 examination. Claudins are considered critical proteins in forming tight junctional complexes in endothelial and epithelial cells and are embedded in the plasma membrane with short cytoplasmic sections that bind to occludin. Owing to multiple isoforms, antibody cross-reactivity can be a significant problem. It was recently shown that a possible misinterpretation of tight junctional claudin-1 localization at the BBB occurred as a result of cross-reactivity of previously available claudin-1 antibody with claudin-3 (68). With use of a new, more selective claudin-1 antibody (catalog no. 51-9000, Zymed) Wolburg and colleagues (68) deduced that claudin-3 is a regular component of the BBB TJs, whereas the presence of claudin-1 in the BBB could not be shown with the reagents available to date. Their examination was

performed with the use of female SJL/N mice. In our laboratory, we were unable to find any expression of claudin-1 with the new, more specific claudin-1 antibody within our rat microvessel preparations, even with the use of immunoprecipitation procedures (data not shown). The claudin-1 antibody with cross-reactivity to claudin-3 has previously produced consistent expression (28, 40). Examination of the new claudin-1 antibody was performed with Madin-Darby canine kidney cells and bovine brain microvessel endothelial cells (cell culture preparations) as well as with our rat brain microvessel isolates (ex vivo) using multiple protein concentrations. Madin-Darby canine kidney and bovine brain microvessel endothelial cells showed claudin-1 expression, whereas no expression was found in the rat brain microvessel isolates. Therefore, claudin-1 expression in BBB TJs may be dependent on species and/or cell lysate preparation. Because our results concurred with those of Wolburg and colleagues (68), we examined claudin-3 expression of the BBB TJ over that of claudin-1.

Occludin, which is a key regulator involved in barrier function (17, 26, 27), was the first tight junctional transmembrane molecule discovered (16). The external loops as well as the transmembrane and the COOH-terminal cytoplasmic domain of occludin are important for regulation of paracellular permeability (4). The COOH-terminal tail of occludin is required for both its localization at the TJ and its direct interaction with ZO-1 protein (17). Under physiological conditions, it is theorized that phosphorylation regulates the maintenance and assembly of TJs (43, 55, 69). Research reports suggest that phosphorylation of occludin regulates tight junctional permeability in a G protein-dependent or -independent manner, depending on the receptor involved, independent of cytoskeletal changes (25). Our data showed occludin (Fig. 6A) expressed as dual bands at 65 kDa ($\beta$-band) and 63 kDa ($\alpha$-band), which are potentially indicative of phosphorylated and nonphosphorylated forms, respectively. At initial H/R (6% $O_2$ for 1 h with 10-min reoxygenation), the occludin $\beta$-band showed a nonsignificant increase, whereas the $\alpha$-band showed a significant decrease. Occludin has been shown to become phosphorylated on serine, threonine, and tyrosine residues (55, 56, 58). Serine and threonine phosphorylation has been theorized to stabilize occludin in its membrane-bound location (7, 14, 55), whereas excessive tyrosine phosphorylation has been theorized to increase transcellular permeability in both epithelial and endothelial cells (12, 19, 58, 66). However, the tyrosine phosphorylation examinations used tyrosine phosphatase inhibitors, which also affect other phosphorylation processes within the cell. Although our examination showed a shift in occludin bands concurrent with the time of functional permeability observed by in situ brain perfusion, further study is required to determine whether this result was actually via phosphorylation, and if so, which residues may have been involved.

This is the first in vivo examination of the BBB under a non-flow-reduced hypoxic insult with assessment of the initial reoxygenation permeability and tight junctional protein expression. We have shown that acute hypoxemia (6% $O_2$ for 1 h) with initial reoxygenation (10 min) produces an increase in BBB permeability associated with alterations in tight junctional protein expression. These results suggest that H/R states lead to reorganization of the TJs and increased paracellular diffusion across the BBB that are not due to increased CBF, vascular volume change, or endothelial uptake of marker. A shift in occludin banding was shown to correlate with changes in functional paracellular permeability without significant change in expression of claudin-3, ZO-1, or actin. Future examination of tight junctional protein change over an extended posthypoxic reoxygenation time course will provide greater insight into mechanisms that underlie BBB alteration as a result of H/R stress.

## REFERENCES

1. **Abbott NJ and Revest PA.** Control of brain endothelial permeability. *Cerebrovasc Brain Metab Rev* 3: 39–72, 1991.
2. **Abbruscato TJ and Davis TP.** Combination of hypoxia/aglycemia compromises in vitro blood-brain barrier integrity. *J Pharmacol Exp Ther* 289: 668–675, 1999.
3. **Bachelard HS, Lewis LD, Ponten U, and Siesjo BK.** Mechanisms activating glycolysis in the brain in arterial hypoxia. *J Neurochem* 22: 395–401, 1974.
4. **Balda MS, Flores-Maldonado C, Cereijido M, and Matter K.** Multiple domains of occludin are involved in the regulation of paracellular permeability. *J Cell Biochem* 78: 85–96, 2000.
5. **Beck T and Krieglstein J.** Cerebral circulation, metabolism, and blood-brain barrier of rats in hypocapnic hypoxia. *Am J Physiol Heart Circ Physiol* 252: H504–H512, 1987.
6. **Butt AM, Jones HC, and Abbott NJ.** Electrical resistance across the blood-brain barrier in anaesthetized rats: a developmental study. *J Physiol* 429: 47–62, 1990.
7. **Clarke H, Soler AP, and Mullin JM.** Protein kinase C activation leads to dephosphorylation of occludin and tight junction permeability increase in LLC-PK1 epithelial cell sheets. *J Cell Sci* 113: 3187–3196, 2000.
8. **Coomber BL and Stewart PA.** Morphometric analysis of CNS microvascular endothelium. *Microvasc Res* 30: 99–115, 1985.
9. **Crawford LE, Milliken EE, Irani K, Zweier JL, Becker LC, Johnson TM, Eissa NT, Crystal RG, Finkel T, and Goldschmidt-Clermont PJ.** Superoxide-mediated actin response in posthypoxic endothelial cells. *J Biol Chem* 271: 26863–26867, 1996.
10. **Crone C and Christensen O.** Electrical resistance of a capillary endothelium. *J Gen Physiol* 77: 349–371, 1981.
11. **Erecinska M and Silver I.** ATP and Brain Function. *J Cereb Blood Flow Metab* 9: 2–19, 1989.
12. **Esser S, Lampugnani MG, Corada M, Dejana E, and Risau W.** Vascular endothelial growth factor induces VE-cadherin tyrosine phosphorylation in endothelial cells. *J Cell Sci* 111: 1853–1865, 1998.
13. **Faquhar MG and PGE.** Junctional complexes in various epithlia. *J Cell Biol* 375–412, 1963.
14. **Farshori P and Kachar B.** Redistribution and phosphorylation of occludin during opening and resealing of tight junctions in cultured epithelial cells. *J Membr Biol* 170: 147–156, 1999.
15. **Furuse M, Fujita K, Hiiragi T, Fujimoto K, and Tsukita S.** Claudin-1 and −2: novel integral membrane proteins localizing at tight junctions with no sequence similarity to occludin. *J Cell Biol* 141: 1539–1550, 1998.

16. **Furuse M, Hirase T, Itoh M, Nagafuchi A, Yonemura S, and Tsukita S.** Occludin: a novel integral membrane protein localizing at tight junctions. *J Cell Biol* 123: 1777–1788, 1993.

17. **Furuse M, Itoh M, Hirase T, Nagafuchi A, Yonemura S, and Tsukita S.** Direct association of occludin with ZO-1 and its possible involvement in the localization of occludin at tight junctions. *J Cell Biol* 127: 1617–1626, 1994.

18. **Gjedde A, Hansen AJ, and Siemkowicz E.** Rapid simultaneous determination of regional blood flow and blood-brain glucose transfer in brain of rat. *Acta Physiol Scand* 108: 321–330, 1980.

19. **Gloor SM, Weber A, Adachi N, and Frei K.** Interleukin-1 modulates protein tyrosine phosphatase activity and permeability of brain endothelial cells. *Biochem Biophys Res Commun* 239: 804–809, 1997.

20. **Gurdjian ES, Stone WE, and Webster JW.** Cerebral metabolism during acute hypoxia. *Arch Neurol Psychiatry* 51: 472–477, 1944.

21. **Hackett PH.** High altitude cerebral edema and acute mountain sickness. A pathophysiology update. *Adv Exp Med Biol* 474: 23–45, 1999.

22. **Haggendal E and Johansson B.** Effects of arterial carbon dioxide tension and oxygen saturation on cerebral blood flow autoregulation in dogs. *Acta Physiol Scand Suppl* 258: 27–53, 1965.

23. **Haskins J, Gu L, Wittchen ES, Hibbard J, and Stevenson BR.** ZO-3, a novel member of the MAGUK protein family found at the tight junction, interacts with ZO-1 and occludin. *J Cell Biol* 141: 199–208, 1998.

24. **Hatashita S and Hoff JT.** Brain edema and cerebrovascular permeability during cerebral ischemia in rats. *Stroke* 21: 582–588, 1990.

25. **Hirase T, Kawashima S, Wong EY, Ueyama T, Rikitake Y, Tsukita S, Yokoyama M, and Staddon JM.** Regulation of tight junction permeability and occludin phosphorylation by Rhoa-p160ROCK-dependent and -independent mechanisms. *J Biol Chem* 276: 10423–10431, 2001.

26. **Hirase T, Staddon JM, Saitou M, Ando-Akatsuka Y, Itoh M, Furuse M, Fujimoto K, Tsukita S, and Rubin LL.** Occludin as a possible determinant of tight junction permeability in endothelial cells. *J Cell Sci* 110: 1603–1613, 1997.

27. **Huber JD, Egleton RD, and Davis TP.** Molecular physiology and pathophysiology of tight junctions in the blood-brain barrier. *Trends Neurosci* 24: 719–725, 2001.

28. **Huber JD, Witt KA, Hom S, Egleton RD, Mark KS, and Davis TP.** Inflammatory pain alters blood-brain barrier permeability and tight junctional protein expression. *Am J Physiol Heart Circ Physiol* 280: H1241–H1248, 2001.

29. **Itoh M, Nagafuchi A, Moroi S, and Tsukita S.** Involvement of ZO-1 in cadherin-based cell adhesion through its direct binding to alpha catenin and actin filaments. *J Cell Biol* 138: 181–192, 1997.

30. **Johannsson H and Siesjo BK.** Blood flow and oxygen consumption of the rat brain in profound hypoxia. *Acta Physiol Scand* 90: 281–282, 1974.

31. **Johannsson H and Siesjo BK.** Cerebral blood flow and oxygen consumption in the rat in hypoxic hypoxia. *Acta Physiol Scand* 93: 269–276, 1975.

32. **Kintner D, Costello DJ, Levin AB, and Gilboe DD.** Brain metabolism after 30 minutes of hypoxic or anoxic perfusion or ischemia. *Am J Physiol Endocrinol Metab* 239: E501–E509, 1980.

33. **Kniesel U and Wolburg H.** Tight junctions of the blood-brain barrier. *Cell Mol Neurobiol* 20: 57–76, 2000.

34. **Krasney J.** Cerebral hemodynamics and high altitude cerebral edema. In: *Hypoxia: Women at Altitude*, edited by Houston C and Coates G. Burlington, VT: Queen City Printers, 1997, p. 254–268.

35. **Krasney JA.** A neurogenic basis for acute altitude illness. *Med Sci Sports Exerc* 26: 195–208, 1994.

36. **Lassen NA and Harper AM.** High-altitude cerebral oedema (Letter). *Lancet* 2: 1154, 1975.

37. **Levine BD, Zhang R, and Roach RC.** Dynamic cerebral autoregulation at high altitude. In: *Hypoxia: Into the Next Mille-nium*, edited by Roach RC, Wagner PD, and Hackett PH. New York: Kluwer Academic/Plenum, 1999, p. 319–322.

38. **Loike JD, Cao L, Brett J, Ogawa S, Silverstein SC, and Stern D.** Hypoxia induces glucose transporter expression in endothelial cells. *Am J Physiol Cell Physiol* 263: C326–C333, 1992.

39. **Lum H, Barr DA, Shaffer JR, Gordon RJ, Ezrin AM, and Malik AB.** Reoxygenation of endothelial cells increases permeability by oxidant-dependent mechanisms. *Circ Res* 70: 991–998, 1992.

40. **Mark KS and Davis TP.** Cerebral microvascular changes in permeability and tight junctions induced by hypoxia-reoxygenation. *Am J Physiol Heart Circ Physiol* 282: H1485–H1494, 2002.

41. **Mitic LL and Anderson JM.** Molecular architecture of tight junctions. *Annu Rev Physiol* 60: 121–142, 1998.

42. **Morita K, Itoh M, Saitou M, Ando-Akatsuka Y, Furuse M, Yoneda K, Imamura S, Fujimoto K, and Tsukita S.** Subcellular distribution of tight junction-associated proteins (occludin, ZO-1, ZO-2) in rodent skin. *J Invest Dermatol* 110: 862–866, 1998.

43. **Nigam SK, Denisenko N, Rodriguez-Boulan E, and Citi S.** The role of phosphorylation in development of tight junctions in cultured renal epithelial (MDCK) cells. *Biochem Biophys Res Commun* 181: 548–553, 1991.

44. **Oldendorf WH and Brown WJ.** Greater number of capillary endothelial cell mitochondria in brain than in muscle. *Proc Soc Exp Biol Med* 149: 736–738, 1975.

45. **Oldendorf WH, Cornford ME, and Brown WJ.** The large apparent work capability of the blood-brain barrier: a study of the mitochondrial content of capillary endothelial cells in brain and other tissues of the rat. *Ann Neurol* 1: 409–417, 1977.

46. **Orr JA, Bisgard GE, Forster HV, Buss DD, Dempsey JA, and Will JA.** Cerebrospinal fluid alkalosis during high altitude sojourn in unanesthetized ponies. *Respir Physiol* 25: 23–37, 1975.

47. **Patlak CS, Blasberg RG, and Fenstermacher JD.** Graphical evaluation of blood-to-brain transfer constants from multiple-time uptake data. *J Cereb Blood Flow Metab* 3: 1–7, 1983.

48. **Payen JF, Fauvage B, Falcon D, and Lavagne P.** [Brain oedema following blood-brain barrier disruption: mechanisms and diagnosis]. *Ann Fr Anesth Reanim* 22: 220–225, 2003.

49. **Plateel M, Dehouck MP, Torpier G, Cecchelli R, and Teissier E.** Hypoxia increases the susceptibility to oxidant stress and the permeability of the blood-brain barrier endothelial cell monolayer. *J Neurochem* 65: 2138–2145, 1995.

50. **Preston JE, al-Sarraf H, and Segal MB.** Permeability of the developing blood-brain barrier to $^{14}C$-mannitol using the rat in situ brain perfusion technique. *Brain Res Dev Brain Res* 87: 69–76, 1995.

51. **Reese TS and Karnovsky MJ.** Fine structural localization of a blood-brain barrier to exogenous peroxidase. *J Cell Biol* 34: 207–217, 1967.

52. **Rosenberg GA.** Ischemic brain edema. *Prog Cardiovasc Dis* 42: 209–216, 1999.

53. **Rothman SM and Olney JW.** Glutamate and the pathophysiology of hypoxic-ischemic brain damage. *Ann Neurol* 19: 105–111, 1986.

54. **Sage JI, Van Uitert RL, and Duffy TE.** Simultaneous measurement of cerebral blood flow and unidirectional movement of substances across the blood-brain barrier: theory, method, and application to leucine. *J Neurochem* 36: 1731–1738, 1981.

55. **Sakakibara A, Furuse M, Saitou M, Ando-Akatsuka Y, and Tsukita S.** Possible involvement of phosphorylation of occludin in tight junction formation. *J Cell Biol* 137: 1393–1401, 1997.

56. **Singer KL, Stevenson BR, Woo PL, and Firestone GL.** Relationship of serine/threonine phosphorylation/dephosphorylation signaling to glucocorticoid regulation of tight junction permeability and ZO-1 distribution in nontransformed mammary epithelial cells. *J Biol Chem* 269: 16108–16115, 1994.

57. **Singh I, Khanna PK, Srivastava MC, Lal M, Roy SB, and Subramanyam CS.** Acute mountain sickness. *N Engl J Med* 280: 175–184, 1969.

58. **Staddon JM, Herrenknecht K, Smales C, and Rubin LL.** Evidence that tyrosine phosphorylation may increase tight junction permeability. *J Cell Sci* 108: 609–619, 1995.

59. **Sutton JR and Lassen N.** Pathophysiology of acute mountain sickness and high-altitude pulmonary oedema: an hypothesis. *Bull Physiopathol Respir (Nancy)* 15: 1045–1052, 1979.

60. **Torbati D, Greenberg JH, and Lambertsen CJ.** Regional cerebral glucose metabolic rate during thirty minutes hypoxia of 7% oxygen in adult conscious rats. *Neurosci Lett* 65: 253–258, 1986.

61. **Triguero D, Buciak J, and Pardridge WM.** Capillary depletion method for quantification of blood-brain barrier transport of circulating peptides and plasma proteins. *J Neurochem* 54: 1882–1888, 1990.

62. **Tsukita S and Furuse M.** Pores in the wall: claudins constitute tight junction strands containing aqueous pores. *J Cell Biol* 149: 13–16, 2000.

63. **Van Itallie CM and Anderson JM.** Occludin confers adhesiveness when expressed in fibroblasts. *J Cell Sci* 110: 1113–1121, 1997.

64. **Vannucci SJ, Seaman LB, and Vannucci RC.** Effects of hypoxia-ischemia on GLUT1 and GLUT3 glucose transporters in immature rat brain. *J Cereb Blood Flow Metab* 16: 77–81, 1996.

65. **Vongsavan N and Matthews B.** Some aspects of the use of laser Doppler flow meters for recording tissue blood flow. *Exp Physiol* 78: 1–14, 1993.

66. **Wachtel M, Frei K, Ehler E, Fontana A, Winterhalter K, and Gloor SM.** Occludin proteolysis and increased permeability in endothelial cells through tyrosine phosphatase inhibition. *J Cell Sci* 112: 4347–4356, 1999.

67. **Wolburg H and Lippoldt A.** Tight junctions of the blood-brain barrier: development, composition and regulation. *Vascul Pharmacol* 38: 323–337, 2002.

68. **Wolburg H, Wolburg-Buchholz K, Kraus J, Rascher-Eggstein G, Liebner S, Hamm S, Duffner F, Grote EH, Risau W, and Engelhardt B.** Localization of claudin-3 in tight junctions of the blood-brain barrier is selectively lost during experimental autoimmune encephalomyelitis and human glioblastoma multiforme. *Acta Neuropathol (Berl)* 105: 586–592, 2003.

69. **Wong V.** Phosphorylation of occludin correlates with occludin localization and function at the tight junction. *Am J Physiol Cell Physiol* 273: C1859–C1867, 1997.

70. **Zaharchuk G, Mandeville JB, Bogdanov AA Jr, Weissleder R, Rosen BR, and Marota JJ.** Cerebrovascular dynamics of autoregulation and hypoperfusion. An MRI study of CBF and changes in total and microvascular cerebral blood volume during hemorrhagic hypotension. *Stroke* 30: 2197–2204; 2204–2205, 1999.

71. **Zhang R, Zuckerman JH, Giller CA, and Levine BD.** Transfer function analysis of dynamic cerebral autoregulation in humans. *Am J Physiol Heart Circ Physiol* 274: H233–H241, 1998.

72. **Zlokovic BV, Begley DJ, Djuricic BM, and Mitrovic DM.** Measurement of solute transport across the blood-brain barrier in the perfused guinea pig brain: method and application to *N*-methyl-alpha-aminoisobutyric acid. *J Neurochem* 46: 1444–1451, 1986.